

# Soft and hard hadronic processes in the nonperturbative approach of QCD

M. N. Sergeenko

*The National Academy of Sciences of Belarus, Institute of Physics, Minsk 220072, Belarus  
and Department of Physics, University of Illinois at Chicago, Chicago, Illinois 60607*

(Received 15 December 1998; revised manuscript received 29 September 1999; published 10 February 2000)

A two-component model to analyze both soft and hard hadronic processes at high energies is suggested. The model is based on the topological  $1/N$  expansion of the scattering amplitude and the theory of the supercritical Pomeron. The longitudinal component is given by the string model and determines the behavior of the cross section on longitudinal variables. The dependence on the transverse momentum is calculated on the basis of a two-gluon Pomeron model in which the Pomeron is modeled as an exchange of two nonperturbative gluons whose propagator is finite at  $q^2=0$ . Hard scattering of quarks on the ends of quark-gluon strings is calculated as a sequence of multi-Pomeron exchanges. It is shown that the propagator which vanishes as  $(q^2)^{-3}$  or faster allows one to reproduce hard distributions of secondary hadrons. The model is used to analyze the inclusive spectra of hadrons on the Feynman variable  $x_F$  and transverse momentum  $p_\perp$  up to 10 GeV/c in a wide energy interval.

PACS number(s): 11.15.Me, 11.15.Pg, 11.15.Tk

## I. INTRODUCTION

It is commonly agreed that all the phenomena of hadron physics should be described in the framework of QCD. There is a simple Lagrangian density of QCD,  $L_{QCD}$ , and in principle everything is derivable from it. But the degrees of freedom in  $L_{QCD}$  are quarks and gluons, not the hadrons we observe in nature. This is why it is not so easy to make quantitative predictions for the real world starting from  $L_{QCD}$ . There are two areas where this has been successful; for short distance phenomena, where perturbation theory can be applied, and for hadron spectroscopy and other long distance phenomena, where numerical or perturbative methods can be applied. There is one more class of phenomena which is neither pure short distance nor pure long distance. These are high-energy hadron-hadron collisions. These reactions are traditionally classified into “hard” and “soft” ones. In hard reactions, all energies and momentum transfers are assumed to be large. In this case the QCD improved parton model describes the reaction of partons by perturbation theory.

As for soft high-energy interactions, the perturbative calculation method is not directly applicable. Instead, most authors develop and apply models that are older of QCD or QCD motivated. Most successful are models based on the Regge approach to high-energy collisions. It was argued in Refs. [1,2] that the conventional Regge approach to high-energy collisions is most probably correct. Regge calculus reproduces many features of hadron interactions at high energy remarkably well. It describes accurately all  $pp$  and  $p\bar{p}$  elastic scattering from the CERN Intersecting Storage Rings (ISR) to Fermilab Tevatron energies, successfully predicts the  $\gamma p$  total cross section [3], diffractive processes and, through optical theorem, the total and inclusive cross sections as well.

To understand many features of hadronic interactions at high energy, it is necessary to introduce a Reggeon known as

the Pomeron. The “soft” Pomeron is responsible for most of the total cross section in hadron-hadron collisions, for small  $-t$  elastic scattering and for diffractive dissociation. In the framework of QCD the Pomeron is understood as the exchange of two (or more) gluons [4]. However the exchange of two perturbative gluons cannot reproduce the experimental results. It was established [5] that the simple phenomenological properties of the Pomeron may readily be understood if the gluon propagator  $D(q^2)$  does not have a singularity at  $q^2=0$ . A behavior softer than a pole of gluon propagator at small  $q^2$  is expected from nonperturbative effects of the QCD vacuum [5], which leads to confinement.

There are several very successful Regge models: dual parton model (DPM) [6], quark-gluon string model (QGSM) [7], VENUS model [8], developed originally to describe soft hadronic interactions, and their modifications [9–11] to describe both soft and semihard hadronic reactions. Within the framework of the DPM, the inclusion of a semihard component has been considered in Ref. [9]. The two-component model embodies the standard DPM for the soft component to which the semihard component was added appropriately. In this model, the partons at the ends of the hard chains get transverse momenta  $p_\perp \geq p_\perp^{cut-off}$  as predicted by perturbative QCD (PQCD).

Another model to analyze soft and semihard hadron processes was suggested in Ref. [11]. The interaction of quarks from colliding hadrons has been calculated as the exchange by nonperturbative (NP) gluons [12], for which the cutoff parameter in the gluonic propagator has been included. The model has allowed us to analyze the inclusive spectra of hadrons in high-energy hadron collisions for transverse momenta up to  $\approx 4$  GeV/c. A similar approach can be used to create a model to analyze data at all available energies for all  $x_F$  and  $p_\perp$ . In this work, we investigate the possibility of reproducing hard distributions of secondary hadrons in the framework of the nonperturbative approach. Using the nonperturbative method, we start with the physics of soft inter-

actions and move as far as possible to the hard region. We develop a two-component model based on the topological  $1/N$  expansion of the scattering amplitude and the “eikonal approximation,” with the use of the conception of the supercritical Pomeron to describe soft and hard hadron distributions at high energy. The longitudinal component is given by the string model in which multi-Pomeron exchanges are represented by the forward scattering diagrams of cylindrical topology and determine the behavior of the cross section on longitudinal variables.

Hard scattering of quarks on the ends of quark-gluon strings is calculated in the multi-Pomeron asymptotic as a sum of multi-gluon exchanges. In these calculations we account for the color interaction between quarks of colliding hadrons before creation and decay of the corresponding strings. The main contribution into such a process at high energy gives a single Pomeron exchange, which is constructed as an exchange of two nonperturbative gluons whose propagator is finite at  $q^2=0$ . Successive multi-Pomeron exchanges required by  $s$  channel unitarity are calculated and give rise to the hard scattering of quarks. We analyze several NP gluon propagators proposed by different authors and observe that the propagator, which vanishes as  $1/q^6$  or faster, in combination with the multi-Pomeron asymptotic of the model, allows us to reproduce hard distributions of secondary hadrons. The model is used to describe data by the Feynman variable  $x_F$  and transverse momentum  $p_\perp$  up to 10 GeV/ $c$ .

## II. THE POMERON

The description of soft hadronic reactions at high energies is in terms of Regge exchanges. A Reggeon known as the Pomeron plays the dominant role in high-energy hadronic reactions. The question is, what is the Pomeron?

There exist different approaches to investigating an object such as the Pomeron [4,13–17]; “soft” and “hard” Pomeron are the most popular of them. The soft Pomeron is constructed from multi-peripheral hadronic exchanges and has intercept  $\alpha_P(0)=1$ . Because this is not compatible with the rising hadronic cross sections at high energies, the soft Pomeron was replaced by a soft supercritical Pomeron with an intercept  $\alpha_P(0)>1$  [15,18].

In the framework of QCD (in the scattering region), the Pomeron is understood as the exchange of two (or more) gluons [4]. The Balitskii-Fadin-Kuraev-Lipatov (BFKL) Pomeron is constructed as an exchange of two perturbative gluons [13,14]. The physics of the soft Pomeron is much less clear. However there is good basis to believe that the soft Pomeron can be considered as an exchange of two nonperturbative gluons whose propagator does not show a pole at  $q^2=0$  [19]. The perturbative approach to the Pomeron has been discussed in Ref. [14]. This approach gives reliable results where the leading logarithmic approximation holds. The hard Lipatov-like Pomeron is built out of multi-peripheral high transverse momentum gluon exchanges and has a series of poles at  $1 < j < 1 + \Delta$  in the complex  $j$  plane. Both the soft supercritical and the hard QCD Pomeron predict a powerlike rise of the total cross section,  $\sigma_{tot}$

$\propto s^{\alpha_P(0)-1}$ . Any realistic perturbative QCD attempts lead to the introduction of an “infrared” cutoff that generates the main part of Pomeron exchange.

A comparative investigation of various Pomeron models was carried out in Ref. [16] in the impact parameter space through their predicted values of  $\sigma_{tot}$ , slope  $B$ , and  $\sigma_{el}/\sigma_{tot}$  in high-energy  $pp$  and  $p\bar{p}$  scattering. It was shown that the data agree with a hybrid eikonal model which combines the hard Lipatov-like QCD Pomeron with the old-fashioned soft Pomeron and Regge terms. The main result of this investigation is that the data is compatible with a smooth transition from a soft to a hard Pomeron contribution which can account for the rise of  $\sigma_{tot}$  with  $s$ .

A connection between the nontrivial vacuum structure of QCD and soft high-energy reactions has been discussed in Refs. [5,20,21]. It was argued [20] that soft collisions should involve in an essential way the NP QCD. A simple model of the vacuum developed by Landshoff and Nachtmann (LN) in Ref. [5] explains the properties of the Pomeron observed in the experiment. In the LN model, Pomeron exchange corresponds to two-gluon exchange.

The starting point of the LN model is that the vacuum consists of a gluon condensate [22],

$$\langle 0 | g^2 : G_{\mu\nu}^b(0) G^{b\mu\nu}(0) : | 0 \rangle = M_c^4, \quad (1)$$

where  $|0\rangle$  denotes the physical nonperturbative vacuum,  $g^2 = 4\pi\alpha_n$  is the QCD coupling constant in nonperturbative regime,  $b=1,2,\dots,8$ , and  $M_c \simeq 1$  GeV. The gluon condensate is characterized by the mass  $M_c$  that measures its magnitude and a finite correlation length,  $a$  [5,23], which are considered as fundamental parameters derivable from the first principles. The Pomeron exchange between quarks behaves like a photon exchange diagram with amplitude  $i\beta_0^2(\bar{u}\gamma_\mu u)(\bar{u}\gamma_\mu u)$ . The strength of the Pomeron coupling to quarks,  $\beta_0$ , is given by

$$\beta_0^2 = \frac{4\pi}{9} \int_0^\infty dk^2 \alpha_n^2 D_{NP}^2(k^2), \quad (2)$$

where  $D_{NP}(k^2)$  is the NP gluon propagator and  $k^2 = -q^2$ . The coupling constant  $\beta_0$  and a mass scale  $\mu_0$  (see below), control the Pomeron form factor. The relationship between the phenomenological parameters of the Pomeron,  $\beta_0$ , and a mass scale  $\mu_0$  and fundamental quantities of NP QCD,  $M_c^4$ , and  $a$  has been established in Ref. [24].

## III. THE NP GLUON PROPAGATOR

The main problem of applicability of perturbative QCD to soft processes comes, as was mentioned in Refs. [25,26], not so much from the size of the coupling but rather from the infrared and collinear singularities emerging from the gluon and quark propagators. Most perturbative calculations need to introduce some kind of regulator as a gluon mass or minimum transverse momentum of the order of 1–3 GeV/ $c$  to give reasonable answers.

The derivation of the NP gluon propagator from QCD [12,26] shows that the low-momentum singularity of the

gauge field propagator is softened. A soft infrared behavior can also be obtained in a Yang-Mills theory with Higgs mechanism, where the gluon acquires a mass, or for some solutions of the Dyson-Schwinger equation [12] or simply in the presence of a cutoff. Hints of a softer behavior at the origin can be found in the lattice calculations (see Ref. [26]). In the Landau [27] and the axial [28] gauge, the gluon propagator seems to behave like that of a massive particle.

Finite gluon condensate requires that the NP gluon propagator,  $D_{NP}(k^2)$ , should be finite at  $k^2=0$ . This is a key requirement of the LN model; the dressed gluon propagator,  $D(k^2)$ , should not have the singularity of the bare massless boson  $\propto 1/k^2$  as  $k^2 \rightarrow 0$ , but should be softened. The singularity in the two-gluon calculation of hadron-hadron scattering is eliminated.

Several such propagators have been considered in the literature [12,17,26,29,30]. The simplest choice is given by the ansatz [30]

$$\alpha_n D_{NP}(k^2) = \frac{3\beta_0}{\sqrt{2\pi}\mu_0} \exp\left(-\frac{k^2}{\mu_0^2}\right), \quad (3)$$

with  $\mu_0 = 1.1$  GeV. This function is required to match the perturbative propagator at a given  $k = Q_0$  that determines  $Q_0$  and  $\alpha_n$ .

A more realistic QCD motivated propagator was obtained in Ref. [12] from the approximate solution of the Dyson-Schwinger equation which contains a dynamically generated gluon mass. In the Feynman gauge this solution is given by  $D_{\mu\nu} = -ig_{\mu\nu}D(k^2)$ , where, in Euclidean space,

$$\alpha_n D(k^2) = \frac{1}{b_0 \ln[(k^2 + 4m_g^2)/\Lambda^2][k^2 + m^2(k^2)]} \quad (4)$$

with momentum dependent dynamical mass given by

$$m^2(k^2) = m_g^2 \left[ \frac{\ln[(k^2 + 4m_g^2)/\Lambda^2]}{\ln(4m_g^2/\Lambda^2)} \right]^{-12/11}. \quad (5)$$

Here in Eqs. (4) and (5)  $b_0 = (33 - 2n_f)/12\pi^2$  and gluon mass  $m_g = 500 \pm 200$  MeV for  $\Lambda = 300$  MeV [12]. The coupling  $\alpha_n$  is frozen in the nonperturbative regime and  $\alpha_n D(k^2)$  is formally independent of  $\alpha_n$ . Solution (4) is valid only for  $m_g > \Lambda/2$  [12]. An important feature of the propagator (4) is that it incorporates the correct ultraviolet behavior, i.e., asymptotically obeys the renormalization group equation. This means that the gluon propagator (4) asymptotically at large  $k^2$  takes the usual form, i.e.,  $D(k^2) \propto 1/k^2$ , because  $m^2(k^2) \rightarrow 0$  at  $k^2 \rightarrow \infty$  and is valid for the entire range of momentum with  $g = 1.5$ .

We analyze these two propagators below in the context of the cross sections they generate in the framework of the model under consideration. We show that the propagator (3) is good only at small  $k^2$ ,  $k^2 \leq 1$  (GeV/c)<sup>2</sup>. Propagator (4) is good in a more wide  $p_\perp$  interval and, in principle, can be used at all  $p_\perp$ . It describes data up to  $p_\perp \approx 3-4$  GeV/c [11], where the nonperturbative effects dominate. However, in the

perturbative region, the calculated cross section goes significantly higher than the experimental data.

This behavior can be explained as follows. The propagator (4) has the perturbative ultraviolet behavior  $D(k^2) \propto 1/k^2$  at  $k^2 \rightarrow \infty$ , which corresponds to one-gluon exchange. But in the perturbative region, one-gluon exchange reproduces the hard scattering of hadrons. Growth of the cross section at  $p_\perp \geq 3$  GeV/c can be explained by the combination of the perturbative behavior of the propagator at large  $k^2$  and the nonperturbative nature of the model, i.e., multiple gluon exchanges which are essential in this region. Therefore some mechanism is required to take into account the nonperturbative effects.

A similar problem has been discussed long ago in Ref. [31]. It was shown that the model obtained by multiplying the usual parton-parton scattering amplitude by the factor

$$B(k^2) = \frac{1}{(k^2 + \mu^2)^2}, \quad (6)$$

where  $\mu \approx 4$  GeV is a parameter (the same for all processes), describes high transverse momentum data from CERN ISR and Fermilab for the processes  $pp \rightarrow cX$  and  $pn \rightarrow cX$  ( $c = \pi^\pm, \pi^0, K^\pm, p, \bar{p}$ ) surprisingly well. The use of the same factor in our model, also, results in the description of high  $p_\perp$  data (see below). The form factor  $B(k^2)$  can be treated as one, which takes into account nonperturbative effects. It results in the dependence  $(k^2)^{-3}$  at  $k^2 \rightarrow \infty$ , if one multiplies the propagator (4) by  $B(k^2)$ . However the factor  $B(k^2)$  contains the scale  $\mu^2 = 16$  GeV<sup>2</sup> which is purely perturbative.

A more rigorous approach which takes into account the nonperturbative effects was developed by Landshoff and Nachtmann in Ref. [5]. They have shown that the complete gluon propagator can be split into a perturbative part,  $\Delta_P(k^2)$ , and a nonperturbative part,  $\Delta_{NP}(k^2)$ , summarizing the vacuum-condensate effects [5] as

$$\langle 0 | T(G_\mu(x) G_\nu(0)) | 0 \rangle = ig_{\mu\nu} \Delta_P(x^2) + ig_{\mu\nu} \Delta_{NP}(x^2). \quad (7)$$

The NP gluon propagator,  $D_{NP}(k^2)$ , leads to the following correlation function for the field strength:

$$\begin{aligned} \langle 0 | : G_{\mu\nu}(x) G^{\mu\nu}(y) : | 0 \rangle \\ = -i \int \frac{d^4 k}{(2\pi)^4} e^{-ik(x-y)} 6k^2 D_{NP}(k^2), \end{aligned} \quad (8)$$

where  $\sqrt{(x-y)^2} = a$  is the correlation length. By setting  $x = y$  one makes contact with the analogue of the Shifman-Vainshtain-Zakharov (SVZ) gluon condensate (1),

$$\begin{aligned} \langle 0 | g^2 : G_{\mu\nu}^b(x) G^{b\mu\nu}(x) : | 0 \rangle \\ \equiv M_c^4 = -ig^2 \int \frac{d^4 k}{(2\pi)^4} 6k^2 D_{NP}(k^2). \end{aligned} \quad (9)$$

Therefore a finite gluon condensate requires  $D_{NP}(k^2)$  to vanish faster than  $(k^2)^{-3}$ .

Consequences of the LN model have been examined in Ref. [25]. It was shown that the LN model based on the analogy Pomeron photon was rather successful. Since then, the LN model has succeeded, at  $t=0$ , in describing the Pomeron in terms of a modified tree-level two-gluon exchange, thus providing a connection with QCD. The basic idea appears to be true; the infrared singularities present in perturbative QCD can be regulated in a process-independent way.

The behavior of the NP propagator  $D_{NP}(k^2)$  at large  $k^2$  can be estimated as follows. According to Eq. (7) the NP propagator  $D_{NP}(k^2)$  can be obtained from the propagator (4) [which is a complete gluon propagator with the asymptotic behavior  $D(k^2) \rightarrow 0$  at  $k^2 \rightarrow \infty$ ] with the help of the subtraction procedure

$$D_{NP}(k^2) = D(k^2) - D_P(k^2), \quad (10)$$

where  $D_P(k^2) = 1/k^2$  is the perturbative gluon propagator. Because of the singularity of  $D_P(k^2)$  at  $k^2=0$  the subtraction procedure makes sense only in the perturbative region, i.e.,  $k^2 > 2-3$  (GeV/c) $^2$ . In this region, the strong coupling  $\alpha_n^2$  in Eq. (4) cannot be taken frozen and the subtraction procedure is very sensitive to the parametrization of  $\alpha_s(k^2)$  at small  $k^2$ . If one chooses the parametrization in the form  $\alpha_s^{-1}(k^2) = b_0 \ln[(k^2 + 4m_g^2)/\Lambda^2]$ , where  $m_g$  is the gluon mass, one obtains, with the help of the subtraction procedure at  $k^2 \geq 3$  (GeV/c) $^2$ , the NP gluon propagator  $D_{NP} \approx (k^2)^{-\nu}$  with  $\nu \approx 3$ .

Therefore the NP gluon propagator  $D_{NP}(k^2)$  and its parameters can be unambiguously fixed. It was found convenient to parametrize the propagator  $D_{NP}(k^2)$  as follows [5]:

$$\alpha_n D_{NP}(k^2) = \frac{M_c^4 a^6}{24\pi} F(k^2 a^2), \quad (11)$$

where dimensionless function  $F$  and correlation length  $a$  are both fixed uniquely by Eqs. (2) and (9). Generalizing the above discussions, we come to the NP gluon propagator

$$\alpha_n D_{NP}(k^2) = \frac{M_c^4 a^6}{24\pi} \frac{1}{(a^2 k^2 + 1)^\nu} \quad (12)$$

with  $\nu = 3 + \epsilon$ . This propagator (incorporated in the model under consideration) gives description of high  $p_\perp$  data (see below) and is in agreement with the LN model for  $\epsilon > 0$ . To guarantee finiteness of the gluon condensate [see Eq. (9)] in accordance with the subtraction procedure, we take  $\epsilon = 0.01$ , though the case with  $\epsilon = 0$  also gives a very good description of the high  $p_\perp$  data. Propagator (12) reproduces the Pomeron coupling (2),  $\beta_0^2 = 3.94$  GeV $^{-2}$ , for  $M_c = 0.993$  GeV and  $a = 0.444$  GeV $^{-1}$  (or 0.08 fm). This fixes the parameters of the NP gluon propagator (12).

#### IV. THE MODEL

The hadron-hadron interactions at high energy are multi-particle processes. Most events consist of the production of a large number of particles with a small transverse moment. For soft processes, the running coupling constant is much too large for ordinary perturbation theory to be applicable. Another feature of hadron interactions is that they involve, in an essential way, multiple gluon exchanges. The amplitude for single quark scattering on each other is not a sensible object (see Ref. [20] and references therein). Sensible objects are the amplitudes for the scattering of hadrons that imply multiple gluon exchanges. The problem is nonperturbative and should involve the corresponding methods. The first step in this way is to use the NP gluon propagator. The second step should involve or effectively account for multiple gluon exchanges. Therefore, alternative nonperturbative methods must be adopted. The theoretical descriptions of measurable quantities like the total cross sections also should involve the NP QCD. It is expected that if the total cross section  $\sigma_{tot}$  has a finite limit as  $s \rightarrow \infty$  then the total cross sections in pure gluonic theory are nonperturbative objects and this conclusion is not changed if  $\sigma_{tot}(s)$  has a logarithmic behavior with  $s$  for  $s \rightarrow \infty$ ,  $\sigma_{tot}(s) \rightarrow \text{const}(\log s)^2$ . This can also be true in full QCD (see Ref. [20]).

The total cross section and the total inelastic cross section of hadron-hadron interaction can be calculated in the framework of the ‘‘eikonal approximation’’ as follows [32]:

$$\sigma_{tot}(s) = \sum_{n=0}^{\infty} \sigma_n(s), \quad (13)$$

$$\sigma_{in}(s) = \sigma^{DD} + \sum_{n=1}^{\infty} \sigma_n(s), \quad (14)$$

where

$$\sigma_n(s) = \frac{\sigma_p}{n\xi} \left( 1 - e^{-\xi \sum_{k=0}^{n-1} \frac{\xi^k}{k!}} \right), \quad n \geq 1 \quad (15)$$

is the cross section for the production of the  $n$  Pomeron chain ( $n$  Pomeron exchange). Here in Eq. (15)

$$\xi = \frac{2C\gamma_p}{R^2 + \alpha'_p(0)\ln(s/s_0)} \left( \frac{s}{s_0} \right)^\Delta, \quad (16)$$

$$\sigma_p = 8\pi\gamma_p \left( \frac{s}{s_0} \right)^\Delta, \quad (17)$$

$\Delta = \alpha_p(0) - 1 \approx 0.08$ ,  $\alpha_p(0)$  is the intercept,  $\alpha'_p(0)$  is the slope of the vacuum trajectory at  $t=0$ ,  $s$  is the squared total energy of colliding hadrons in the c.m.s., and  $s_0 = 1$  GeV $^2$ . The parameter  $C = 1 - \sigma^{DD}/\sigma_{el}$  accounts for the deviation from the eikonal approximation and  $\sigma^{DD}$  is the total cross section of diffraction dissociation. The cross section  $\sigma_p$  is the contribution of the supercritical Pomeron [15,18] to the total cross section, parameters  $\gamma_p = 3.45$  GeV $^{-2}$ , and  $R^2 = 2.77$  GeV $^{-2}$  ( $pp$  interaction) and determine the value of



the Pomeron coupling with a hadron. The sum of the topological cross sections,  $\sigma_n$ , yields the total cross section for inclusive reactions [see Eqs. (13) and (14)]. This means that the quantities  $\sigma_n$  contain in integrated form all the information about the process under consideration, i.e., soft interactions, hard interactions, etc. This fact can be used to determine the invariant inclusive cross section,  $F(x_F, \vec{p}_\perp)$ , in the framework of the nonperturbative approach.

At the present time, the best one can do in describing nonperturbative phenomena is to construct models which incorporate all available theoretical ideas. One widely studied nonperturbative approach consists of taking various large  $N$  limits of QCD, where  $N$  can be either the number of colors  $N_c$  or the number of flavors  $N_f$  [33]. This approach, which is known as dual topological unitarization (DTU) [33,34], has allowed us to establish the connection between Feynman diagrams and certain geometrical objects like planar diagrams, cylindrical diagrams, etc. The Pomeron singularity in this approach corresponds to the first term of topological  $1/N$  expansion. The next terms correspond to multi-Pomeron exchanges, which are the most important feature we use in our model.

There are several very successful models based on the topological  $1/N$  expansion of the scattering amplitude; DPM [6], QGSM [7], and the VENUS model [8] for very energy nuclear scattering. In the QGSM, the multiple production of hadrons at high energies is described by “cutting” the forward scattering diagrams of the “cylindrical” type [7]. Each cylinder corresponds to the exchange of a single Pomeron. For the production of a hadron  $h$  in hadron-hadron scattering, the cross section corresponding to graphs of the cylinder-cut type is written in the form [7]

$$f(x) \equiv \int E \frac{d\sigma}{d^3p} d^2\vec{p}_\perp = \sum_{n=0}^{\infty} \sigma_n(s) \phi_n^h(x), \quad (18)$$

where  $\sigma_n$  is the cross section of the  $n$  Pomeron exchange that corresponds to the creation of  $2n$   $q(q\bar{q})$  (or  $q\bar{q}$ ) strings decaying into secondary hadrons and the function  $\phi_n^h(x)$  describes the  $x$  distribution of hadron  $h$  produced from the decay of the  $2n$  strings created in the  $n$  Pomeron-exchange process.

There are some versions of the DPM [9] and QGSM [10,11,35] which account for the transverse moments of quarks in initial hadrons. These models have allowed us to describe the two-dimensional inclusive spectra of hadrons produced in hadron-hadron, hadron-nucleus, and nucleus-nucleus collisions at different energies. In particular, the Monte Carlo version of the DPM [9] allows us to describe the  $p_\perp$  distribution of both produced stable particles and resonances.

The QGSM is usually limited by the analysis of soft hadronic reactions and we use its basic features in the longitudinal component of our model. For soft hadronic processes, quark distributions over the longitudinal variable  $x$  on the ends of  $q\bar{q}$  strings are found from the Regge asymptotic of graphs (cylinder or planar type) at  $x \rightarrow 0$  and 1 [7]. The decay of each of this strings into hadrons is described by hadroni-

zation functions, the form of which is determined by the Regge asymptotic of these graphs too [7].

Consider a hadron production in the hadron-nucleon collision at high energy including the transverse motion of quarks in colliding hadrons in the framework of the nonperturbative approach. The Pomeron exchange corresponding to the cylindrical graph can be represented as the exchange of two NP gluons as follows. Each of the two colliding hadrons is divided into a quark and diquark (antiquark) with the opposite transverse moments. After the color interaction between quarks of the hadrons by means of NP gluons, two strings are created in the chromostatic constant field. These two strings then decay into secondary hadrons. In the framework of  $1/N$  expansion of the scattering amplitude, the process is repeated  $n$  times during the  $n$  Pomeron exchange. The main contribution to such processes at large energies gives the graphs of cylinder-cut type in the  $s$  channel which correspond to the multiple Pomeron exchanges in the  $t$  channel [6–8]. Successive multiple gluon exchanges result in the increase of the transverse moments of quarks on the ends of strings that is analogous to the so-called successive division of energy between the  $2n$  quark-gluon strings in the multiperipheral model of hadron production [7].

The invariant inclusive hadron spectrum corresponding to these diagrams can be written in the following form<sup>1</sup> [10,11]:

$$F(x, \vec{p}_\perp) \equiv E \frac{d\sigma}{d^3p} = \sum_{n=0}^{\infty} \sigma_n(s) \phi_n^h(x, \vec{p}_\perp), \quad (19)$$

where  $\sigma_n$  is the topological cross section and the function  $\phi_n^h(x, \vec{p}_\perp)$  describes the  $x$  and  $p_\perp$  distribution of hadrons produced from the decay of the  $2n$  strings. The term with  $n = 0$  corresponds to diffraction dissociation. The distributions  $\phi_n^h(x, \vec{p}_\perp)$  are written in terms of the light-cone variables.

Light-cone quantization of quantum field theory has emerged as a promising method for solving problems in the strong coupling regime. This method has a number of unique features. It seems to be well suited to solving QCD and, contrary to other approaches, the relativistic wave functions transform trivially to a boosted frame. Moreover, its language is close to experiment and phenomenology. An important general feature of the behavior of the light-cone wave function is that each Fock component describes a system of free particles [36,37]. This feature is especially important in our further consideration.

The functions  $\phi_n^h(x, \vec{p}_\perp)$  in Eq. (19) can be written in the form

$$\phi_n^h(x, \vec{p}_\perp) = \int_{x_+}^1 dx_1 \int_{x_-}^1 dx_2 \psi_n^h(x, \vec{p}_\perp; x_1, x_2), \quad (20)$$

<sup>1</sup>As an example, we consider here the production of hadron  $h$  in the nucleon-nucleon collision. In case of meson-nucleon scattering one needs to replace the diquark from the projectile nucleon by the antiquark from the meson,  $qq \rightarrow \bar{q}$ , in the formulas.

where

$$\begin{aligned}\psi_n^h(x, \vec{p}_\perp; x_1, x_2) &= \mathcal{F}_n^{qq}(x_+, \vec{p}_\perp; x_1) \tilde{\mathcal{F}}_n^q(x_-, \vec{p}_\perp; x_2) \\ &+ \mathcal{F}_n^q(x_+, \vec{p}_\perp; x_1) \tilde{\mathcal{F}}_n^{qq}(x_-, \vec{p}_\perp; x_2) \\ &+ 2(n-1) \mathcal{F}_n^{q_{sea}}(x_+, \vec{p}_\perp; x_1) \\ &\times \tilde{\mathcal{F}}_n^{q_{sea}}(x_-, \vec{p}_\perp; x_2).\end{aligned}\quad (21)$$

Here  $x_\pm = \frac{1}{2}[(x_\perp^2 + x_n^2)^{1/2} \pm x_n]$  are the light-cone variables in the  $n$  Pomeron chain,  $x_\perp = 2[(m_h^2 + \vec{p}_\perp^2)/s]^{1/2}$ ,  $x_1, x_2$  are the longitudinal coordinates of quarks on the ends of the string, and  $m_h$  is the mass of the secondary hadron  $h$ .

There are several methods to calculate the functions  $\phi_n^h(x, \vec{p}_\perp)$  [18]. As we show below, in our approach transverse momentum between the Pomeron showers is divided successively. In this case the functions  $\phi_n^h(x, \vec{p}_\perp)$  are written in the form

$$\phi_n^h(x, \vec{p}_\perp) = \sum_{k=1}^n \phi_k^h(x_k, \vec{p}_\perp), \quad (22)$$

where the longitudinal variable  $x$  in the  $n$ th chain depends on the  $n$  [7];  $x_n = x/(1-x_0)^{n-1}$ ,  $x_0 \approx 0.35$ . The functions  $\mathcal{F}_n^\tau(x_+, \vec{p}_\perp; x_1)$ , where  $\tau = q, \bar{q}, qq, q_{sea}, \bar{q}_{sea}$ , are the probabilities of production of the hadron  $h$  from the fragmentation of the upper ends of the strings (beam fragmentation) and the functions

$$\tilde{\mathcal{F}}_n^\tau(x_-, \vec{p}_\perp; x_2) = \mathcal{F}_n^\tau(x_-, \vec{p}_\perp; x_2) / \tilde{\mathcal{F}}_n^\tau(0, \vec{p}_\perp) \quad (23)$$

are the probabilities of production of the hadron  $h$  from the fragmentation of the lower ends (target fragmentation). These functions are represented by the convolutions

$$\mathcal{F}_n^\tau(x_\pm, \vec{p}_\perp; x_{1,2}) = \int d^2\vec{k}_\perp \tilde{\mathcal{F}}_n^{\tau,h}(x_{1,2}, \vec{k}_\perp) \tilde{G}_{\tau \rightarrow h}\left(\frac{x_\pm}{x_{1,2}}, \vec{k}_\perp; \vec{p}_\perp\right), \quad (24)$$

$$\tilde{\mathcal{F}}_n^\tau(0, \vec{p}_\perp) = \int_0^1 dx' \int d^2\vec{k}_\perp \tilde{\mathcal{F}}_n^{\tau,h}(x', \vec{k}_\perp) \tilde{G}_{\tau \rightarrow h}(0, \vec{p}_\perp). \quad (25)$$

The quark distributions in the initial hadrons over  $x$  and  $k_\perp$  can be taken in the factorized form [11,35], i.e.,

$$\tilde{f}_0^{\tau,h}(x, \vec{k}_\perp) = f_0^{\tau,h}(x) g_0(\vec{k}_\perp), \quad (26)$$

where  $f_0^{\tau,h}(x)$  is the quark  $x$  distribution in the initial hadron, which has the form  $f_0^{\tau,h}(x) = Cx^\alpha(1-x)^\beta$  [7,18], and  $g_0(\vec{k}_\perp)$  is quark  $k_\perp$  distribution in initial hadron. The factorized form (26) will also be true after the  $n$  gluon exchange

$$\tilde{f}_n^{\tau,h}(x, \vec{k}_\perp) = f_n^{\tau,h}(x) g_n(\vec{k}_\perp). \quad (27)$$

The hadronization functions  $\tilde{G}_{\tau \rightarrow h}(z, \vec{k}_\perp; \vec{p}_\perp)$  have been taken in the form [10]

$$\tilde{G}_{\tau \rightarrow h}(z, \vec{k}_\perp; \vec{p}_\perp) = G_{\tau \rightarrow h}(z) \tilde{g}(\vec{k}_\perp), \quad (28)$$

where

$$\tilde{g}(\vec{k}_\perp) = \frac{\tilde{\gamma}}{\pi} \exp(-\tilde{\gamma} \vec{k}_\perp^2), \quad \vec{k}_\perp = \vec{p}_\perp - z \vec{k}_\perp, \quad z = \frac{x_\pm}{x_{1,2}}. \quad (29)$$

The functions  $G_{\tau \rightarrow h}(z)$  on the right hand side of Eq. (28) describe  $z$  dependence of the hadronization of the quark  $\tau$  into the hadron  $h$ ; these functions have the form [38]

$$G_{\tau \rightarrow h}(z) = a_h(1-z)^{\eta(\tau,h)+\lambda} f(z). \quad (30)$$

Quantities  $\eta(\tau, h)$  and  $f(z)$  depend on the type of reaction. The functions  $G_{\tau \rightarrow h}(z)$  and their parameters have been described in detail in Ref. [38]. For the fragmentation  $u \rightarrow \pi^+$  (favored fragmentation) they are, for example,  $\eta(u, \pi^+) = -\alpha_\rho(0)$  and  $f(z) = 1$ , and for  $d \rightarrow \pi^+$  (unfavored fragmentation) we have  $\eta(u, \pi^+) = -\alpha_\rho(0) + 1$  and  $f(z) = 1$ . Here  $\alpha_\rho(0)$  is the intercept of the leading  $\rho$  Regge trajectory corresponding to light  $u$  and  $d$  quarks. Parameter  $\lambda = 2\alpha'_h(0)\langle p_\perp^2 \rangle$ , where  $\alpha'_h(0)$  and  $\langle p_\perp^2 \rangle$  are the intercept of the leading Regge trajectory and the average squared transverse momentum of the secondary hadron  $h$ , respectively. The parameter  $\lambda \approx 0.5$  is considered as an universal one, i.e., it is the same for all reactions. This gives, for example, an estimation of  $\langle p_\perp^2 \rangle$  if we know intercept  $\alpha'_h(0)$ . (Intercepts and slopes of meson Regge trajectories have been calculated in Ref. [39] in the framework of the quark potential model with QCD motivated potential.) The functions  $\mathcal{F}_n^\tau(x_+, \vec{p}_\perp; x_1)$  give dominant contribution into the cross section at  $x > 0$  [ $\approx 97\%$  with respect to  $\tilde{\mathcal{F}}_n^\tau(x_-, \vec{p}_\perp; x_2)$ ]. In this case light-cone variable  $x_- \approx 0$ . On the contrary, the functions  $\tilde{\mathcal{F}}_n^\tau(x_-, \vec{p}_\perp; x_2)$  give the dominant contribution at  $x < 0$  ( $x_+ \approx 0$ ). This essentially simplifies calculations and formulas without a loss of accuracy if one considers the regions  $x > 0$  or  $x < 0$  separately. For instance, for the reaction  $\pi^+ N \rightarrow hX$  we have, for  $x > 0$  (beam fragmentation),

$$\begin{aligned}\phi_n^h(x, \vec{p}_\perp) &= \int_{x_+}^1 dx_1 \left[ f_n^{u,h}(x_1) G_{u \rightarrow h}\left(\frac{x_+}{x_1}\right) I_n\left(\frac{x_+}{x_1}, \vec{p}_\perp\right) + f_n^{\bar{d},h}(x_1) G_{\bar{d} \rightarrow h}\left(\frac{x_+}{x_1}\right) I_1(z, \vec{p}_\perp) \right. \\ &\quad \left. + f_n^{u_{sea},h}(x_1) G_{u_{sea} \rightarrow h}\left(\frac{x_+}{x_1}\right) \sum_{k=2}^n I_k\left(\frac{x_+}{x_1}, \vec{p}_\perp\right) + f_n^{\bar{d}_{sea},h}(x_1) G_{\bar{d}_{sea} \rightarrow h}\left(\frac{x_+}{x_1}\right) \sum_{k=1}^{n-1} I_k\left(\frac{x_+}{x_1}, \vec{p}_\perp\right) + \varphi_{DD}(x_1) g_{DD}(\vec{p}_\perp) \right],\end{aligned}\quad (31)$$

where

$$I_n(z, \vec{p}_\perp) = \int d^2\vec{k}_\perp g_n(\vec{k}_\perp) \tilde{g}_{\tau \rightarrow h}(\vec{p}_\perp - z\vec{k}_\perp) \quad (32)$$

and the functions  $\varphi_{DD}(x_1)$  and  $g_{DD}(\vec{p}_\perp)$  describe diffraction dissociation [10,18].

## V. QUARK $k_\perp$ DISTRIBUTIONS

Pomeron exchange is a soft process. However the capability of the model under consideration to calculate the contribution of multi-Pomeron exchanges allows us to reproduce hard scattering of quarks on the ends of quark-gluon strings as a sequence of multi-Pomeron exchanges.

The functions  $g_n(\vec{k}_\perp)$  in the above formulas describe the quark  $k_\perp$  distributions on the ends of strings after  $n$  Pomeron exchange between colliding hadrons, which reduces to the color interaction between constituents of these hadrons. We calculate these functions as the convolutions of the quark distributions in initial hadrons,  $g_0(\vec{k}_\perp)$ , with the square of the NP quark-quark scattering amplitude.

(1) Initial quark distributions,  $g_0(\vec{k}_\perp)$ , can be calculated with the help of hadronic wave functions ( $wf$ ). The hadronic  $wf$  are underlying links between hadronic phenomena in QCD at large distances (nonperturbative) and small distances (perturbative). To be successive we have to use the nonperturbative  $wf$  appropriate at small transverse moments. The NP  $wf$  in QCD have been introduced to the theory to describe the exclusive processes [40]. The main idea of this approach is the separation of the large and small distances physics. At small distances one can use the standard perturbative expansion. All nontrivial, large distance physics is hidden into NP  $wf$  and cannot be found by the perturbative technique.

Large distance phenomena are controlled by the confining linear potential. The  $wf$  for this potential was obtained from an approximate bound-state solution in the quark models for hadrons [41] and the exact solution for harmonic-oscillator interaction in the framework of the Poincare-invariant quantum mechanics [42],

$$\psi_{c.m.}(\vec{q}^2) = A \exp\left(-\frac{\vec{q}^2}{2\beta^2}\right). \quad (33)$$

There is a possible connection between the rest frame  $wf$  (33) and the light-cone  $wf$ ,  $\psi_{LC}(x, \vec{k}_\perp)$  [43],

$$\psi_{c.m.}(\vec{q}^2) \leftrightarrow \psi_{LC}(x, \vec{k}_\perp). \quad (34)$$

An important general feature of the behavior of the light-cone wave function is that each Fock component describes a system of free particles with kinematics invariant mass squared [36,37]

$$M^2 = \sum_i^n \frac{\vec{k}_{iT}^2 + m_i^2}{x_i}. \quad (35)$$

This feature is essentially exploited in our model.

The solution for two particles bound in a harmonic oscillator potential can be taken as a model for the light-cone wave function,  $\psi_{LC}(x, \vec{k}_\perp^2)$ , for quarks in the confining linear potential. In order to get the Lorentz invariant light-cone wave function, we use the Brodsky-Huang-Lepage prescription for the harmonic wave functions [36],

$$\psi_{LC}(x, \vec{k}_\perp^2) = A \exp\left(-b \sum_i^n \frac{\vec{k}_{iT}^2 + m_i^2}{x_i}\right), \quad (36)$$

where  $b = 1/6\alpha^2$  for nucleon,  $b = 1/8\beta^2$  for pion, and  $n$  is the number of particles in the bound state. The same behavior is also true for asymptotically large  $\vec{k}_\perp^2$ ,  $\vec{k}_\perp^2 \rightarrow \infty$  [44]. It was shown in Ref. [45] that with the universal scale  $\alpha \approx \beta \approx 320$  MeV and constituent quark masses  $m = 330$  MeV all static properties of the nucleon and pion but the charge radius of the neutron are described to an accuracy of 10%.

The quark distribution on the end of a string can be calculated as follows. Wave function (36) can be written in the factorized form

$$\psi_{LC}(x, \vec{k}_\perp^2) = \prod_i^n A_i \exp\left(-b \frac{\vec{k}_{iT}^2 + m_i^2}{x_i}\right), \quad (37)$$

where each factor corresponds to a separate particle. Quark  $k_\perp$  distribution on the end of a string can be calculated for some average  $x$ ,  $\langle x \rangle$ . Using the fact that the convolution of two Gaussian distributions gives again Gaussian distribution, we obtain, for the quark distribution on the end of the string,

$$g_0(\vec{k}_\perp) = C \exp(-\gamma \vec{k}_\perp^2), \quad (38)$$

where  $\gamma = 1/\langle \vec{k}_\perp^2 \rangle$  and  $\langle \vec{k}_\perp^2 \rangle$  is the average squared transverse momentum of quarks inside the hadron. To estimate  $\langle \vec{k}_\perp^2 \rangle$  we assume the hadronic  $wf$  peaked at  $x \approx \frac{1}{3}$  [19]. Then for  $\langle \vec{k}_\perp^2 \rangle$  in the nucleon we estimate  $\langle \vec{k}_\perp^2 \rangle \approx 6\alpha^2 \langle x \rangle = 0.18$  (GeV/c)<sup>2</sup>. The constant  $C = \gamma/\pi$  is determined from the normalization condition

$$\int g_0(\vec{k}_\perp) d^2\vec{k}_\perp = 1. \quad (39)$$

Therefore the initial quark  $k_\perp$  distribution on the end of string can be taken in the Gaussian form normalized to 1.

(2) The next important ingredient we have to estimate is the NP quark-quark scattering amplitude. In order to determine the scattering amplitude in the infrared limit one needs information about the nonperturbative behavior of gluons, i.e., in this limit, nonperturbative aspects of QCD are crucial [20,26]. Explicit calculations for high-energy elastic hadron-hadron scattering near the forward direction [20] support the idea that the vacuum structure of QCD plays an essential role in soft high-energy scattering.

As was shown in Refs. [20,21] the  $qq$  scattering is a NP process and the scattering amplitude can be obtained by first calculating the amplitudes for each quark in an external gluonic potential. In a second step one has to average the product of the corresponding scattering amplitudes over all gluon

potentials with an appropriate functional integral measure. The result obtained in Ref. [21] apparently shows that one has to take the whole sum of gluon interactions of two quark lines and average them. In these calculations the nonperturbative ansatz for the gluon propagator should be used.

To find the NP  $qq$  scattering amplitude we consider elastic proton-proton scattering via the Pomeron exchange in which the Pomeron is constructed as an exchange of two NP gluons. The amplitude for elastic proton-proton scattering via two-gluon exchange can be written as [46] (see, also, Ref. [19])

$$A(s, t) = 8is\alpha_s^2 [T_1 - T_2]. \quad (40)$$

Here  $T_1$  represents contributions from diagrams where both gluons are attached to the same quark within the proton, whereas  $T_2$  comes from diagrams in which the gluons are attached to different quarks. Analysis of the data from the total cross sections, elastic scattering, and inelastic diffraction dissociation strongly suggests that the Pomeron couples to single quarks and to a good approximation behaves like a  $C=1$  isoscalar photon [5].

Perturbative exchange of two gluons does not reproduce the  $t$  dependence if the gluons couple to different quarks and is obtained naturally when one makes the gluons couple to single quarks. There is a contribution from diagrams in which the two gluons do not couple to the same quark. This provides a partial cancellation which is complete in the limit of zero hadron radius [46].

This fact is particularly important for our purpose of extracting the  $qq$  scattering amplitude via two NP gluon exchange; for the scattering of two pointlike quarks, formula (40) can be simplified by the taking into account only the term  $T_1$ ,

$$T_1 = \int_0^s d^2q D_{NP}[(q+k/2)^2] D_{NP}[(q-k/2)^2] F_1(t), \quad (41)$$

where the electromagnetic form factor  $F_1(t) = 1$  for the scattering of point-like particles and  $t = -k^2$ . Therefore, we can consider the NP quark-quark scattering amplitude of the form

$$A_{NP}(s, t) = isK\alpha_n^2 \int_0^s d^2q D_{NP}[(q+k/2)^2] D_{NP}[(q-k/2)^2], \quad (42)$$

where  $K$  is a constant factor,  $\alpha_n$  is the strong running coupling constant in the nonperturbative regime, and  $D_{NP}(k^2)$  is the NP gluon propagator (12). The convolution function then can be taken in the form of the scattering amplitude squared,  $A_{NP}^2(k^2)$ .

The quark distribution  $g_1(\vec{k})$  on the end of the string after one-Pomeron exchange can be calculated with the help of the formula

$$g_1(\vec{k}_\perp) = \int d^2\vec{k}'_\perp A_{NP}^2[(\vec{k}'_\perp - \vec{k}_\perp)^2] g_0(\vec{k}'_\perp). \quad (43)$$

The distribution functions  $g_2(\vec{k}_\perp)$ ,  $g_3(\vec{k}_\perp)$ , etc., are calculated analogously to the above case. This means that the quark distribution  $g_2(\vec{k}_\perp)$  is obtained after exchange by the second Pomeron in the corresponding chain; this distribution will be expressed via the function  $g_1(\vec{k}_\perp)$ ,

$$g_2(\vec{k}_\perp) = \int d^2\vec{k}'_\perp A_{NP}^2[(\vec{k}'_\perp - \vec{k}_\perp)^2] g_1(\vec{k}'_\perp). \quad (44)$$

Repeating this iteration procedure  $n$  times, we obtain the quark distribution function  $g_n(\vec{k}_\perp)$  in the  $n$ th chain expressed via the function  $g_{n-1}(\vec{k}_\perp)$  and, therefore, via the function  $g_0(\vec{k}_\perp)$  as

$$\begin{aligned} g_n(\vec{k}_\perp) &= \int d^2\vec{k}_{\perp, n-1} A_{NP}^2[(\vec{k}_{\perp, n-1} - \vec{k}_\perp)^2] g_{n-1}(\vec{k}_{\perp, n-1}) \\ &= \int d^2\vec{k}_{\perp, n-1} A_{NP}^2[(\vec{k}_{\perp, n-1} - \vec{k}_\perp)^2] \\ &\quad \times \int d^2\vec{k}_{\perp, n-2} A_{NP}^2[(\vec{k}_{\perp, n-2} - \vec{k}_{\perp, n-1})^2] \cdots \\ &\quad \times \int d^2\vec{k}_{\perp, 0} A_{NP}^2[(\vec{k}_{\perp, 0} - \vec{k}_{\perp, 1})^2] g_0(\vec{k}_{\perp, 0}). \end{aligned} \quad (45)$$

Note that if  $n$  is the number of Pomeron exchanges we take into account in a given reaction, then  $\vec{k}_\perp = \vec{k}_{\perp, n}$ .

The distribution functions  $f_n^{\tau, h}(x)$  can be calculated with the help of the regular or successive division of  $x$  between  $2n$   $q\bar{q}$  chains [18]. In this work, we use the successive division of  $x$ , which corresponds to the  $k_\perp$  division arising (by product) in our approach as a result of the successive gluon exchanges.

This method of calculation of the successive NP gluon exchanges effectively results in the hard distribution of quarks on the ends of  $q\bar{q}$  string. The sensitivity of the distributions  $g_n(\vec{k}_\perp)$  to the choice of the form of  $g_0(\vec{k}_\perp)$  is very weak because of the strong dependence of the NP scattering amplitude (42) on  $q^2$ . This method of calculation of the  $k_\perp$  distributions of quarks on the ends of strings allows us to reproduce the inclusive spectra  $F(x, \vec{p}_\perp)$  of secondary hadrons over  $x$  and  $p_\perp$  up to  $p_\perp \approx 10$  GeV/ $c$ .

## VI. RESULTS AND DISCUSSIONS

One-Pomeron exchange plays the dominant role in high-energy hadronic reactions. However, with the energy growth, multiple Pomeron exchanges begin to play an important role. The model developed in this work represents a natural framework to calculate such processes. In Fig. 1, we show the mean number of the exchanged Pomerons in the  $pp$  interaction as the function of  $\sqrt{s}$ . As one might expect the function  $\langle N_P \rangle(\sqrt{s})$  grows with  $\sqrt{s}$ , i.e., the contribution of multi-Pomeron exchange processes becomes more and more important with the energy growth. It is interesting to emphasize that the  $\langle N_P \rangle(\sqrt{s})$  is between 1 and 3 up to TeV energies. Figure 2 represents the distributions of quarks on the



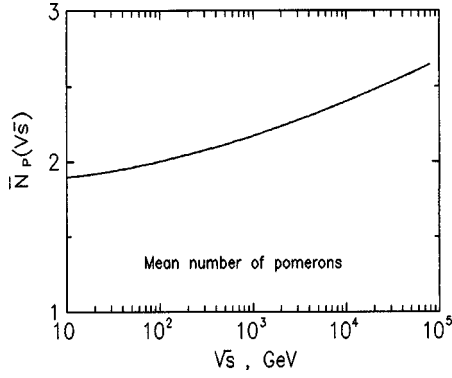


FIG. 1. Average number of the exchanged Pomerons in  $pp$  interaction as the function of  $\sqrt{s}$  [the solid curve here and on other plots below shows the calculation result with the propagator (12)].

ends of the quark-gluon strings,  $g_n(\vec{k}_\perp)$ , for different  $n$ . These distributions are harder for larger  $n$ .

Using the formula (19), we can calculate many characteristics of the hadron production at high energies; invariant distributions, differential and total cross sections, asymmetry of  $D$  meson production, multiplicities of hadrons, correlation of the average transverse momentum  $\langle p_\perp \rangle$  on multiplicity of hadrons, multiplicity distributions, etc. [10]. Invariant distribution  $f(x)$  and  $p_\perp$  distribution can be calculated with the help of the formulas

$$f(x) = \int F(x, \vec{p}_\perp) d^2 \vec{p}_\perp, \quad (46)$$

$$\frac{d\sigma}{dp_\perp^2} = \pi \frac{\sqrt{s}}{2} \int F(x, \vec{p}_\perp) \frac{dx}{E^*}, \quad (47)$$

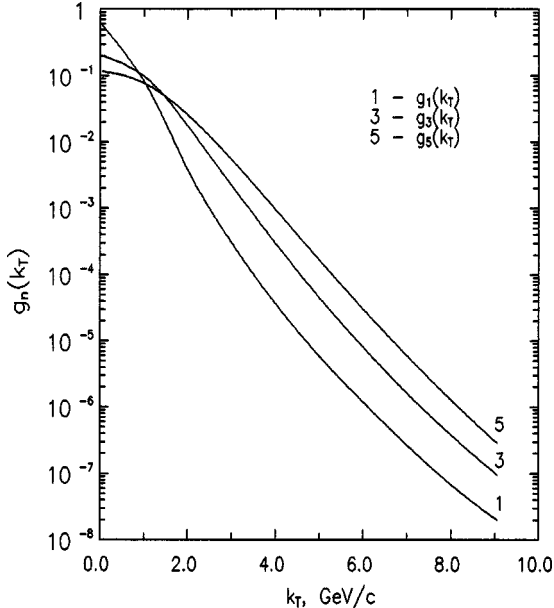


FIG. 2. Distributions of quarks on the ends of the quark-gluon strings as the function of the internal transverse momentum  $k_\perp$  for  $n=1$ ,  $n=3$ , and  $n=5$ .

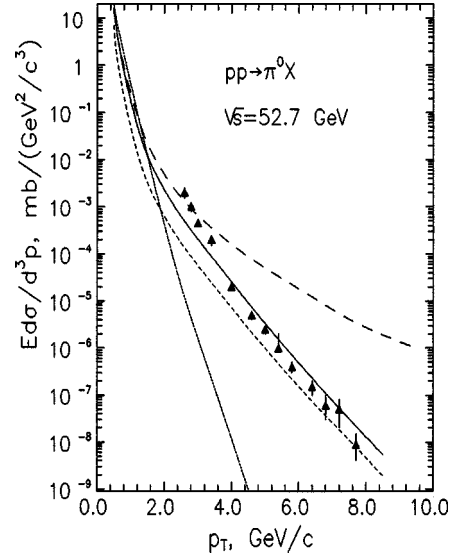


FIG. 3. The inclusive cross section of the reaction  $pp \rightarrow \pi^0 X$  versus transverse momentum at  $\sqrt{s}=52.7$  GeV. The solid curve shows the calculation result with the propagator (12), the dotted line with the Gaussian propagator (3), and the dashed line above the data has been obtained with the use of the Cornwall's propagator (4). The small dashed line shows one Pomeron contribution into cross section ( $n=1$ ) with the propagator (12). The data are from Ref. [47].

where  $E^*$  is the energy of the hadron  $h$  in the c.m.s. of the reaction and  $F(x, \vec{p}_\perp)$  is given by Eq. (19).

The calculation results of different physical characteristics of hadrons produced in hadron-nucleon collisions are shown in Figs. 3–11. In Fig. 3, we show the invariant cross section  $E(d\sigma/d^3 p)$  versus transverse momentum  $p_\perp$  for the  $\pi^0$  me-

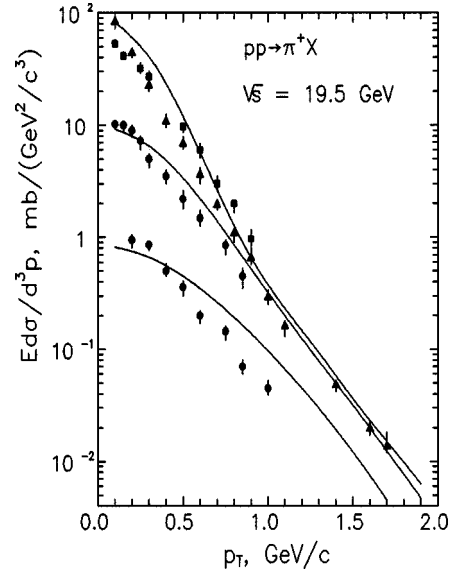


FIG. 4. Invariant cross section  $F(x, \vec{p}_\perp^2)$  of  $\pi^+$  mesons produced in reaction  $pp \rightarrow \pi^+ X$  at  $p_0=200$  GeV/c as a function of  $p_\perp$  for the different values of  $x$ ,  $x=0$ ,  $0.3$ , and  $0.6$ . Experimental data are from Refs. [48].

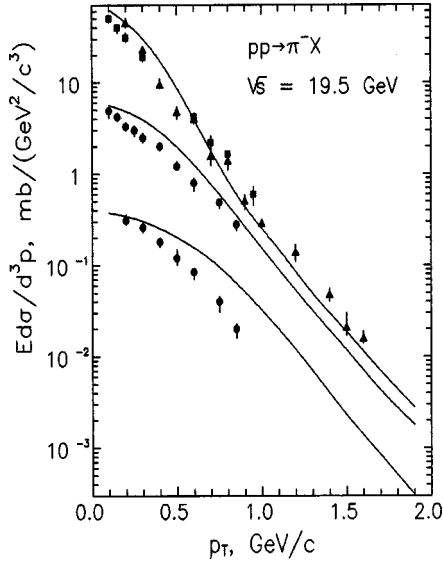


FIG. 5. Invariant cross section  $F(x, p_{\perp}^2)$  of  $\pi^-$  mesons produced in reaction  $pp \rightarrow \pi^- X$  at  $p_0 = 200$  GeV/c as a function of  $p_{\perp}$  for the different values of  $x$ ,  $x = 0, 0.3$ , and  $0.6$ . Experimental data are from Refs. [48].

sons produced in  $pp$  collisions at  $\sqrt{s} = 52.7$  GeV and  $x = 0$ . Curves correspond to the calculation results obtained with the use of the propagators considered in Sec. III. We see a good description (solid line) of data [47] up to  $p_{\perp} \approx 10$  GeV/c with the propagator (12).

Parameter  $\gamma = 1/\langle k_{\perp}^2 \rangle$  is defined by the average squared transverse momentum of quarks inside a hadron. For a nucleon, we estimate  $\langle k_{\perp}^2 \rangle \approx 0.18$  (GeV/c) $^2$  (see Sec. IV). This parameter is the same for all processes at all energies. Parameter  $\tilde{\gamma}$  [see Eq. (29)],  $\tilde{\gamma} = 1/\langle p_{\perp}^2 \rangle$ , where  $\langle p_{\perp}^2 \rangle$  is the average squared transverse momentum of the secondary hadron. For  $\pi$  meson production, we estimate  $\langle p_{\perp}^2 \rangle$

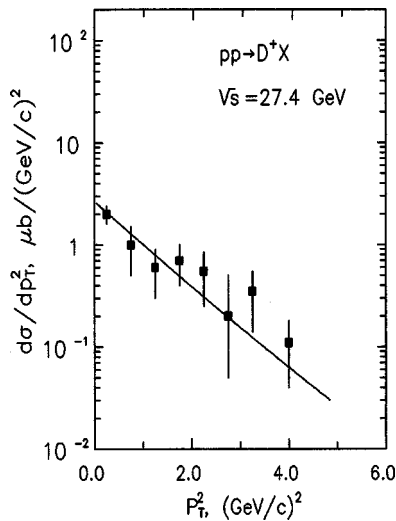


FIG. 6. Differential cross sections of the reaction  $pp \rightarrow D^+ X$  at the energy  $\sqrt{s} = 27.4$  GeV as a function of  $p_{\perp}^2$ . The curve corresponds to calculation with the intercept  $\alpha_{\psi}(0) = 0$ . The data are from Ref. [49].

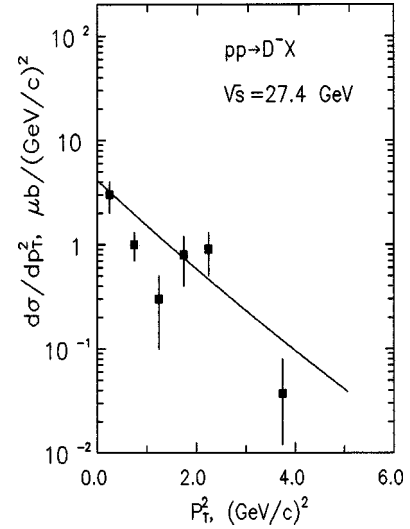


FIG. 7. Differential cross sections of the reaction  $pp \rightarrow D^- X$  at the energy  $\sqrt{s} = 27.4$  GeV as a function of  $p_{\perp}^2$ . The curve corresponds to calculation with the intercept  $\alpha_{\psi}(0) = 0$ . The data are from Ref. [49].

$\approx 0.2$  (GeV/c) $^2$ . Values of the parameters for some reactions are given in Table I. In this table, parameters  $\gamma_p$  and  $R^2$  determine the value of the Pomeron coupling with a hadron [see Eqs. (13)–(17)]; these parameters depend only on the type of initial particles. Parameters  $a_h$  and  $\tilde{\gamma}$  enter into hadronization functions  $G(z, \vec{k}_{\perp}, \vec{p}_{\perp})$  [see Eqs. (28)–(30)]; they depend on the type of secondary particles.

In Figs. 4 and 5 we show the invariant cross section  $E(d\sigma/d^3\vec{p})$  of  $\pi^+$  and  $\pi^-$  mesons produced in  $pp$  collisions at  $p_{lab} = 200$  GeV/c as a function of  $p_{\perp}$  for three different values of the Feynman variable  $x_F$ :  $x_F = 0, 0.3$ , and  $0.6$ . We see a good agreement of the model prediction with the experimental data [48]. In Figs. 6–12 we demonstrate the possibility of the model for description of  $D$  meson spectra. We show the calculation results for the differential cross sections

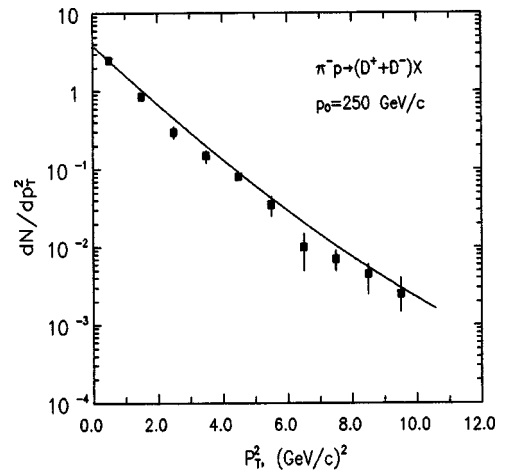


FIG. 8. The combined  $D^+ p_{\perp}^2$  data from E769 [52] is compared to our calculation integrated over  $0.4 < x_F < 1$ . The curve corresponds to calculation with the intercept  $\alpha_{\psi}(0) = 0$ .

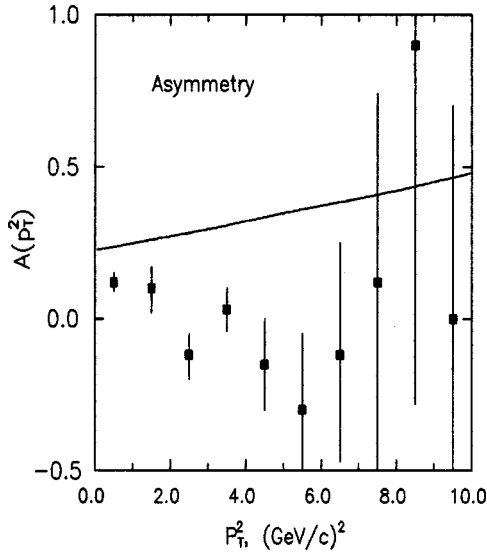


FIG. 9. The  $x_F$  integrated ( $0.1 < x_F < 0.7$ ) asymmetry of  $D$  meson production in  $\pi^- p$  interaction of E769 [52] at  $p_0 = 250$  GeV/c.

$d\sigma/dp_\perp^2$  of the reactions  $pp \rightarrow D^\pm X$  at  $\sqrt{s} = 27.4$  GeV. The curves correspond to the case when the Regge  $\psi$  trajectory has the intercept  $\alpha_\psi(0) \approx 0$  that presupposes nonlinear  $\psi$  trajectory [39]. From this figure, one can see a good agreement of the model prediction with the experimental data for  $D$  mesons [49]. The inclusive spectra of  $D^\pm$  mesons have been calculated for the parameter  $\tilde{\gamma} = 0.9$  (GeV/c) $^{-2}$  in hadronization functions, which corresponds to the average squared transverse momentum of the secondary  $D$  mesons,  $\langle p_\perp^2 \rangle \approx 1.11$  (GeV/c) $^2$ .

Experiments at Fermilab and CERN have observed a strong asymmetry between the hadroproduction cross sections of leading  $D$  mesons, containing projectile valence quarks, and nonleading charmed mesons without projectile valence quarks [50]. In  $\pi^-$  interactions with hadrons or nu-

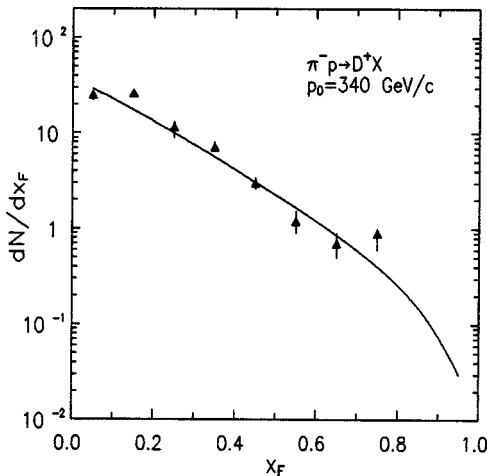


FIG. 10. The  $x_F$  distribution for nonleading charm production in the reaction  $\pi^- p \rightarrow D^+ X$  at  $p_0 = 340$  GeV/c compared with the WA82 data [52].

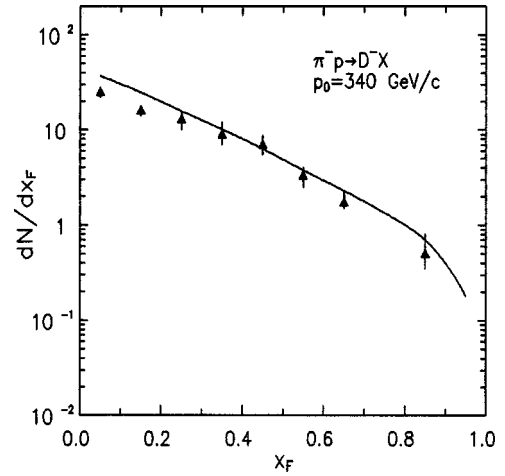


FIG. 11. The  $x_F$  distribution for leading charm production in the reaction  $\pi^- p \rightarrow D^- X$  at  $p_0 = 340$  GeV/c compared with the WA82 data [52].

clei, the  $D^-$   $x_F$  distribution is consistently harder than the  $D^+$  distribution. The  $D^-$  and  $D^0$  are referred to as “leading” charmed mesons while the  $D^+$  and  $\bar{D}^0$  are nonleading. The observed correlation of the  $\pi^\pm N \rightarrow D^\pm X$  cross sections with the projectile charge violates the usual assumption that heavy quark jet fragmentation factorizes.

The asymmetry between leading and nonleading charm particles is defined as

$$A = \frac{\sigma(\text{lead}) - \sigma(\text{nonlead})}{\sigma(\text{lead}) + \sigma(\text{nonlead})}. \quad (48)$$

In Ref. [51], the asymmetry as a function of  $x_F$  and  $p_\perp^2$  has been examined assuming a two-component model combining leading-twist fusion subprocesses and charm production from intrinsic heavy quark Fock states. The magnitude and kinematics dependence of the asymmetry is explained in this model by an intrinsic  $c\bar{c}$  production cross section of  $0.5 \mu\text{b}$ .

In our model, a sizable leading charm asymmetry is predicted by the charm hadronization mechanisms incorporated in the hadronization functions. The calculation results for  $\pi^- p$  interaction are shown in Fig. 8. The hadronization functions  $G_{q \rightarrow h}(z)$  of quark (diquarks) chains into charmed mesons are determined as  $z \rightarrow 1$  by the intercept of the  $c\bar{c}$  Regge trajectory,  $\alpha_\psi(0)$  [38]. The main uncertainty of the calculations comes from poor knowledge of the intercept of  $\psi$  trajectory,  $\alpha_\psi(0)$ . Unfortunately, the large number of errors in charm cross section measurement at  $\sqrt{s} = 630$  GeV

TABLE I. The model parameters for some reactions.

Reaction	$\gamma_p$ , GeV $^{-2}$	$R^2$ , GeV $^{-2}$	$a_h$	$\tilde{\gamma}$ , (GeV/c) $^{-2}$
$\pi p \rightarrow \pi X$	2.27	2.23	0.43	5.0
$\pi p \rightarrow DX$	2.27	2.23	$10^{-4}$	0.90
$pp \rightarrow \pi X$	3.43	2.77	0.45	5.0
$pp \rightarrow KX$	3.45	2.77	0.05	3.81
$pp \rightarrow DX$	3.45	2.77	$10^{-4}$	0.90

does not allow one to extract a useful constant for the  $\alpha_\psi(0)$ . Comparison of the calculations with data shows a good agreement for the case when  $\psi$  trajectory has intercept  $\alpha_\psi(0) \approx 0$ . Such a value of the intercept corresponds to the nonlinear  $\psi$  trajectory calculated in Ref. [39].

If one assumes the leading  $c\bar{c}$  trajectory to be nonlinear (on what indicates many quark models; see, for example, [39] and references therein) and the parameters of the  $\alpha_\psi(t)$  are dictated by the perturbation theory of QCD, then  $\alpha_\psi(0) \approx 0$ . For the fragmentation of the  $d$  quark chain into  $D^-$  mesons (favored fragmentation), for instance, the function  $G(z)$  is [38]

$$G_{d \rightarrow D^-}(z) = a_D(1-z)^{-\alpha_\psi(0)+\lambda}(1+b_D z^2), \quad (49)$$

and the hadronization function of the  $d$  quark into  $D^+$  mesons (unfavored fragmentation) is

$$G_{d \rightarrow D^+}(z) = a_0^D(1-z)^{-\alpha_\psi(0)+\lambda+2[1-\alpha_R(0)]}. \quad (50)$$

Here  $\alpha_R(0) \approx 0.5$ ,  $\alpha_\psi(0) \approx 0$  are the intercepts of the  $\rho$  meson and  $\psi$  Regge trajectories, respectively,  $a_D = 0.110^{-3}$ ,  $b_D = 5$ . Favored fragmentation corresponds to leading quark fragmentation and unfavored to nonleading. The complete list of the hadronization functions is given in Ref. [38].

In Fig. 9 we show the  $x_F$ -integrated ( $0.1 < x_F < 0.7$ ) asymmetry of  $D$  meson production in  $\pi^- p$  interaction of E769 [52] at  $p_0 = 250$  GeV/c. In Figs. 10 and 11 we compare the calculation results with the  $x_F$  distributions for nonleading charm (Fig. 10), leading charm distributions (Fig. 11), and the asymmetry (Fig. 12) in  $\pi^- p$  interaction at  $p_0 = 340$  GeV/c with the WA82 [52] data. The calculations show a good agreement with data.

## VII. CONCLUSION

Hard processes can be explained by the PQCD and models containing the semihard component. The main question that should be considered in this work is whether it is possible to apply the nonperturbative approach based on  $1/N$  expansion of the scattering amplitude and the “eikonal approximation” to analyze the hard hadronic processes.

To deal with such a possibility we have used the fact that the first term of the topological  $1/N$  expansion corresponds to the Pomeron singularity and the next terms correspond to multi-Pomeron exchanges. In this work, we have developed a nonperturbative model to describe both soft and hard distributions of hadrons at high energies. For this we have used the fact that the total cross section and the total inelastic cross section of hadron-hadron interactions can be calculated in the framework of the “eikonal approximation” as the sum of the topological cross sections,  $\sigma_n$ , which give weights of the corresponding  $n$  Pomeron-exchange diagrams. The longitudinal component is given by the string model in which the  $n$  Pomeron exchange is modeled by the forward scattering diagrams of the cylindrical type.

According to Low and Nussinov we have modeled the Pomeron as the two-gluon exchange, but we have modeled the exchange of two nonperturbative gluons as suggested by

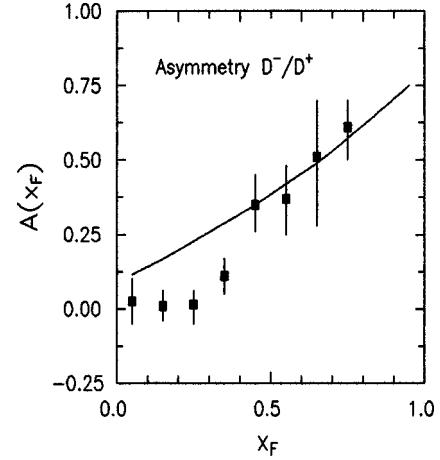


FIG. 12. The  $p_\perp$  integrated asymmetry of  $D$  meson production of E769 [52] at  $p_0 = 340$  GeV/c.

Landshoff and Nachtmann. The most important ingredient of the transverse component of our model is the NP gluon propagator. We have analyzed several propagators proposed by different authors and shown that the Gaussian-type propagator (3) is good only at small  $k^2$ ,  $k^2 \leq 1$  (GeV/c)<sup>2</sup>. Cornwall’s propagator (4) can be used (in the framework of the approach under consideration) at small  $p_\perp$  up to  $p_\perp \approx 3-4$  GeV/c, where nonperturbative effects dominate, and fails to describe data at  $p_\perp > 4$  GeV/c [11].

We have dealt with Cornwall’s propagator in the context of the Landshoff-Nachtmann model and extracted the “pure” NP propagator. We have shown that the last one which vanishes as  $\propto 1/q^6$  or faster, in combination with the multi-Pomeron asymptotic of the model, can reproduce the soft and hard distributions of secondary hadrons. The propagator suggested reproduces the Pomeron coupling  $\beta_0^2$ ,  $\beta_0^2 = 3.94$  GeV<sup>-2</sup> for the value of the gluon condensate  $M_c = 0.993$  GeV and the correlation length  $a = 0.444$  GeV<sup>-1</sup> that allowed us to fix parameters of the NP gluon propagator.

To calculate soft and hard hadronic processes, we have taken into account the dependence of quark distributions in colliding hadrons and the quark hadronization functions on the transverse momentum  $k_\perp$ . The color interaction of valence quarks, diquarks, and sea quarks (antiquarks) of the hadrons has been taken into account.

Contrary to the simple one-gluon-exchange picture for hard scattering, in our approach the transverse momentum of quarks on the ends of  $n$  Pomeron strings is a result of the sum of multiple gluon exchanges. The quark distribution functions,  $g_n(\vec{k}_\perp)$ , are calculated iteratively as the convolutions of the initial quark distribution,  $g_0(\vec{k}_\perp)$ , with the squared NP scattering amplitude,  $A_{NP}^2(q^2)$ , corresponding to the exchange by two NP gluons. This calculation procedure results in hard distributions of quarks on the ends of the strings and corresponds to successive division of the internal transverse momentum  $k_\perp$  and longitudinal variable  $x$  between  $2n$  chains ( $2n$  quark-gluon strings).

The model has been developed to calculate invariant distributions  $F(x, \vec{p}_\perp)$  for inclusive hadronic reactions. Self-consistency of the model is demonstrated by a good agree-



ment of  $x$  and  $p_{\perp}$  distributions of secondary hadrons which are obtained by integration of invariant distribution  $F(x, \vec{p}_{\perp})$ . The model provides a reasonable description of inclusive spectra of protons,  $\pi$ ,  $K$ ,  $D$ , and  $B$  mesons in hadron collisions at high energy for all  $x$  and transverse moments up to 10 GeV/ $c$ , for the same parameter values at all energies. The essential parameters of the transverse component of the model, the value of the gluon condensate  $M_c$  and the correlation length  $a$ , are both fixed by normalization conditions for the NP gluon propagator and can be calculated from the first principles.

## ACKNOWLEDGMENTS

The author thanks Professor Uday P. Sukhatme for the kind invitation to visit the University of Illinois at Chicago where a part of the work was done and, also, for useful discussions and valuable comments. I should also like to thank Professor A.A. Bogush and Professor A.B. Kaidalov for support and constant interest in this work, and Dr. G.I. Lykasov and Dr. G. Arakelyan for numerous useful discussions. This work was supported in part by the Belarusian Fund for Fundamental Researches.

- 
- [1] A. Donnachie and P. V. Landshoff, Part. World **2**(1), 7 (1991).
  - [2] J. Bjorken, SLAC-PUB-6477, 1994; F. Halzen, MAD/PH/772, Madison, 1993.
  - [3] A. Donnachie and P. V. Landshoff, Phys. Lett. B **296**, 227 (1992); Nucl. Phys. **B267**, 690 (1986); **B244**, 322 (1984); **B267**, 1690 (1985).
  - [4] F. E. Low, Phys. Rev. D **12**, 163 (1975); S. Nussinov, Phys. Rev. Lett. **34**, 1286 (1975).
  - [5] P. V. Landshoff and O. Nachtmann, Z. Phys. C **35**, 405 (1987).
  - [6] A. Capella, U. Sukhatme, C.-I. Tan, and J. Tran Thanh Van, Phys. Rep. **236**, 228 (1994); A. Capella, U. Sukhatme, and J. Tran Thanh Van, Z. Phys. C **3**, 329 (1980); A. Capella, U. Sukhatme, C.-I. Tan, and J. Tran Thanh Van, Phys. Lett. **81B**, 68 (1979); G. Cohen-Tannoudji, El Hassouni, J. Kalinowski, O. Napoli, and R. Peschanski, Phys. Rev. D **21**, 2699 (1980); P. Aurenche and F. W. Bopp, Phys. Lett. **114B**, 363 (1982).
  - [7] A. B. Kaidalov, Phys. Lett. **116B**, 459 (1982); A. B. Kaidalov and K. A. Ter-Martirosyan, *ibid.* **117B**, 247 (1982).
  - [8] K. Werner, Phys. Rep. **232**, 87 (1993).
  - [9] J. Ranft, Z. Phys. C **27**, 413 (1985); D. Petermann, J. Ranft, and F. W. Bopp, *ibid.* **54**, 682 (1992).
  - [10] G. I. Lykasov and M. N. Sergeenko, Z. Phys. C **52**, 635 (1991); **56**, 697 (1992); Yad. Fiz. **55**, 2502 (1992) [Sov. J. Nucl. Phys. **55**, 1393 (1992)].
  - [11] G. I. Lykasov and M. N. Sergeenko, Z. Phys. C **70**, 455 (1996).
  - [12] J. M. Cornwall, Phys. Rev. D **26**, 1453 (1982).
  - [13] V. S. Fadin, E. A. Kuraev, and L. N. Lipatov, Zh. Éksp. Teor. Fiz. **72**, 377 (1977) [Sov. Phys. JETP **45**, 199 (1977)]; Y. Y. Balitski and L. N. Lipatov, Yad. Fiz. **28**, 1597 (1978) [Sov. J. Nucl. Phys. **28**, 822 (1978)].
  - [14] L. N. Lipatov, Yad. Fiz. **23**, 642 (1976) [Sov. J. Nucl. Phys. **23**, 338 (1976)]; Zh. Éksp. Teor. Fiz. **90**, 1536 (1986) [Sov. Phys. JETP **63**, 904 (1986)].
  - [15] P. V. Landshoff and O. Nachtmann, Z. Phys. C **35**, 405 (1987).
  - [16] E. Gotsman, E. M. Levin, and U. Maor, Z. Phys. C **57**, 677 (1993).
  - [17] L. Jenkovszky, A. Kotikov, and F. Paccanoni, Z. Phys. C **63**, 131 (1994).
  - [18] A. B. Kaidalov and K. A. Ter-Martirosyan, Yad. Fiz. **39**, 1545 (1984) [Sov. J. Nucl. Phys. **39**, 979 (1984)]; **40**, 211 (1984) [**40**, 135 (1984)].
  - [19] F. Halzen, G. I. Krein, and A. A. Natale, Phys. Rev. D **47**, 295 (1993).
  - [20] O. Nachtmann, "Nonperturbative QCD Effects in High Energy Collisions," Talk presented at the 18th Johns Hopkins Workshop, Florence, Italy, 1994, HD-THEP-94-42, 1994.
  - [21] O. Nachtmann, Ann. Phys. (N.Y.) **209**, 436 (1991); A. Krämer and H. G. Dosch, Phys. Lett. B **252**, 669 (1991).
  - [22] M. A. Shifman, A. I. Vainshtein, and V. I. Zakharov, Pis'ma Zh. Éksp. Teor. Fiz. **27**, 60 (1978) [JETP Lett. **27**, 55 (1978)]; Nucl. Phys. **B147**, 385 (1979); **B147**, 448 (1979); **B147**, 519 (1979).
  - [23] H. G. Dosch and Yu. A. Simonov, Phys. Lett. B **205**, 339 (1988); Yu. A. Simonov, Nucl. Phys. **B307**, 512 (1988).
  - [24] A. Donnachie and P. V. Landshoff, Nucl. Phys. **B311**, 509 (1988).
  - [25] J. R. Cudell, Nucl. Phys. **B336**, 1 (1990).
  - [26] J. R. Cudell and D. A. Ross, Nucl. Phys. **B359**, 247 (1991).
  - [27] J. E. Mandula and M. Ogilvie, Phys. Lett. B **185**, 127 (1987).
  - [28] P. A. Amundsen and J. Greensite, Phys. Lett. B **173**, 179 (1986).
  - [29] S. Mandelstam, Phys. Rev. D **20**, 3223 (1979); M. Baker, J. S. Ball, and F. Zachariasen, Nucl. Phys. **B186**, 531 (1981); **B186**, 560 (1981); N. Brown and M. R. Pennington, Phys. Rev. D **38**, 2266 (1988); **39**, 2723 (1989).
  - [30] J. R. Cudell, Nucl. Phys. **B336**, 1 (1990).
  - [31] E. Fischbach and G. W. Look, Phys. Rev. D **15**, 2576 (1977).
  - [32] K. A. Ter-Martirosian, Phys. Lett. **44B**, 377 (1973).
  - [33] G. 't Hooft, Nucl. Phys. **B72**, 461 (1974); G. Veneziano, Phys. Lett. **52B**, 220 (1974); Nucl. Phys. **B74**, 365 (1974); **B117**, 519 (1976); E. Witten, *ibid.* **B160**, 57 (1979).
  - [34] C. F. Chew and C. Rosenzweig, Phys. Rep. **41**, 263 (1978); Chan Hong-Mo *et al.*, Nucl. Phys. **B86**, 470 (1975); **B92**, 13 (1975).
  - [35] A. I. Veselov, O. I. Piskounova, and K. A. Ter-Martirosyan, ITEP-176, 1984.
  - [36] G. P. Lepage, S. J. Brodsky, T. Huang, and P. B. Mackensie, Proceedings of the Banff Summer Institute, 1981; S. J. Brodsky, Gary McCartor, H.-C. Pauli, and S. Pinsky, SLAC-PUB-5811, OHSTPY-HEP-T-92-005, 1992.
  - [37] S. J. Brodsky, T. Huang, and G. P. Lepage, in *Particles and Fields*, edited by A. Z. Carpi and A. N. Kamal (Plenum, New York, 1983).
  - [38] A. B. Kaidalov and O. I. Piskunova, Yad. Fiz. **43**, 1545 (1986) [Sov. J. Nucl. Phys. **43**, 994 (1986)].

- [39] M. N. Sergeenko, Z. Phys. C **64**, 315 (1994).
- [40] S. J. Brodski and G. P. Lepage, in *Perturbative Quantum Chromodynamics*, edited by A. H. Mueller (World Scientific, Singapore, 1989); V. Chernyak and A. R. Zhitnitsky, Phys. Rep. **112**, 173 (1984); S. Brodski and G. P. Lepage, Phys. Lett. **87B**, 359 (1979); V. Chernyak and A. R. Zhitnitsky, Pis'ma Zh. Eksp. Teor. Fiz. **25**, 544 (1977) [JETP Lett. **25**, 510 (1977)]; A. Duncan and A. H. Mueller, Phys. Rev. D **21**, 1636 (1980).
- [41] See, e.g., Elementary Particle Theory Group, Acta Phys. Sin. **25**, 415 (1976).
- [42] V. V. Andreev and M. N. Sergeenko, UIC, UICHEP-TH/99-6, Chicago, Illinois, 1999.
- [43] Tao Huang, Bo-Qiang Ma, and Qi-Xing Shen, Phys. Rev. D **49**, 1490 (1994).
- [44] A. R. Zhitnitsky, Phys. Lett. B **375**, 211 (1995).
- [45] Z. Dziembowski, Phys. Rev. D **37**, 778 (1988).
- [46] J. F. Gunion and D. E. Soper, Phys. Rev. D **15**, 2617 (1977); E. M. Levin and M. G. Ryskin, Yad. Fiz. **34**, 1114 (1981) [Sov. J. Nucl. Phys. **34**, 619 (1981)]; Balitsky and Lipatov (Ref. [13]); D. G. Richard, Nucl. Phys. **B258**, 267 (1985).
- [47] F. W. Busser *et al.*, Phys. Lett. **46B**, 471 (1973).
- [48] A. E. Brenner *et al.*, Phys. Rev. D **26**, 1497 (1982); P. Capiiluppi *et al.*, Nucl. Phys. **B70**, 1 (1974).
- [49] M. Aguilar-Benitez *et al.*, Phys. Lett. B **201**, 176 (1988); Z. Phys. C **40**, 321 (1988).
- [50] M. Aguilar-Benitez *et al.*, Phys. Lett. **161B**, 400 (1985); Z. Phys. C **31**, 491 (1986).
- [51] R. Vogt and S.J. Brodsky, SLAC-PUB-6468, LBL-35380, 1994.
- [52] G. A. Alves *et al.*, Phys. Rev. Lett. **69**, 3147 (1992); **72**, 812 (1994); M. Adamovich *et al.*, Phys. Lett. B **305**, 402 (1993).